

Magnetic exchange mechanism for electronic gap opening in graphene

T. G. Rappoport¹, M. Godoy^{1,2}, B. Uchoa³, R. R dos Santos¹ and A. H. Castro Neto⁴

¹*Instituto de Física, Universidade Federal do Rio de Janeiro,
CP 68.528, 21941-972 Rio de Janeiro RJ, Brazil*

²*Instituto de Física, Universidade Federal de Mato Grosso, 78060-900, Cuiabá MT, Brazil.*

³*Department of Physics, University of Illinois at Urbana-Champaign, 1110 W. Green St, Urbana, IL, 61801, USA and*

⁴*Department of Physics, Boston University, 590 Commonwealth Avenue, Boston, MA 02215, USA*

(Dated: Version 11.1 – October 31, 2018)

We show within a local self-consistent mean-field treatment that a random distribution of magnetic adatoms can open a robust gap in the electronic spectrum of graphene. The electronic gap results from the localization of the charge carriers that arises from the interplay between the graphene sublattice structure and the exchange interaction between the adatoms. The size of the gap depends on the strength of the exchange interaction between carriers and localized spins and can be controlled by both temperature and external magnetic field. Furthermore, we show that an external magnetic field creates an imbalance of spin-up and spin-down carriers at the Fermi level, making doped graphene suitable for spin injection and other spintronic applications.

PACS numbers: 71.27.+a, 73.20.Hb, 75.30.Hx

Graphene is a two-dimensional sheet of carbon atoms whose elementary excitations are massless Dirac fermions [1]. Due to the vanishing density of states (DOS) near the Dirac points, adatoms, such as H, which are otherwise non-magnetic and bond strongly to carbon atoms, can easily form local magnetic moments in graphene [2, 3].

The combination of properties such as ballistic transport, extremely large spin coherence lengths [4], and gating effects makes this material very attractive for spintronic applications [5].

For certain applications, such as in the fabrication of transistors, it would be desirable to open a large gap in graphene. However, opening a gap in suspended samples has turned out to be unexpectedly difficult. Dirac fermions have long inelastic mean free paths and are typically insensitive to disorder and localization effects. The Dirac points seem also very robust against instabilities in general. In this Letter, we show that the adsorption of magnetic adatoms constitutes a surprisingly flexible way to open a controllable gap in graphene.

For a random distribution of adatoms sitting on top of carbon sites, the sublattice quantum numbers in graphene are such that at low densities, two spins lying on different sublattices interact antiferromagnetically, whereas for spins on the same sublattice the interaction is ferromagnetic [6–8]. Due to the nature of this magnetic interaction, for full lattice coverage (that is, one adatom per carbon, $n_s = 1$), the system is antiferromagnetic, whereas for low values of n_s , there is a competition between the AFM and FM interactions, giving rise to the formation of spin textures and clusters [9]. As we will show, these magnetic textures can localize charge carriers in graphene.

We address this issue by considering a tight-binding model, in which local magnetic moments are randomly distributed on a honeycomb lattice, and interact with the spin of the itinerant electrons through a local Heisen-

berg exchange interaction; this effective interaction results from the interplay between hybridization effects and Coulomb interactions, similarly to the Kondo Hamiltonian for metals [10].

Within a mean-field approach, which takes into account the positional disorder of localized spins [11, 12], we are able to discuss the magnetic and electronic properties of the system as functions of temperature, external magnetic field, and density of localized spins; we are also able to examine the electronic density of states, which displays a gap driven by the exchange coupling and the magnetic properties of the localized spins. As a result, we find a gap which can be controlled by temperature and external magnetic field.

We start from a random distribution of magnetic impurities (or spins) sitting on top of carbon atoms. For spins on top carbon sites, the exchange Hamiltonian in graphene has a simple form [13], and the total Hamiltonian, including charge carriers and external fields, is

$$\mathcal{H} = -t \sum_{\langle i,j \rangle} (a_{i\sigma}^\dagger b_{j\sigma} + h.c.) + \sum_i J_i \vec{S}_i \cdot \vec{s}_i - g\mu_B H \sum_i s_i^z - \tilde{g}\mu_B H \sum_i S_i^z, \quad (1)$$

where $a_{i\sigma}$ ($b_{i\sigma}$) annihilates an electron with spin σ on site i of sublattice $\alpha = A$ (B). The first term in Eq. (1) describes charge carriers hopping between nearest neighbor graphene sites, with $t \simeq 2.7$ eV while the second one couples localized (\vec{S}_i) and itinerant (\vec{s}_i) spins through the local exchange constant $J_i > 0$; the last two terms in Eq. (1) describe the interaction of the carriers and spins with an external *in-plane* magnetic field H . Although the exchange interaction is local, the indirect interaction among the localized spins is long ranged, which, in principle, allows the formation of a true ordered state in two dimensions, in spite of thermal fluctuations.

The exchange interaction is treated within a mean-field approximation, $\vec{S}_i \cdot \vec{s}_i \rightarrow S(i)s_i^z + S_i^z s(i) - S(i)s(i)$, where the magnetizations $S(i) \equiv \langle S_i^z \rangle$ and $s(i) \equiv \langle s_i^z \rangle$ must be computed self-consistently at each site [11, 12]. The mean-field decomposition results in an effective Hamiltonian of charge carriers that can be fully diagonalized for any configuration of localized spins. We then calculate the expectation value of the carrier spins $s(j)$ on all lattice sites. The expectation value of each *local* spin can be computed back by enforcing $S(i)$ to be equal to the local magnetization due to charge carriers at each impurity site, in the presence of the external field, $S(i) = \mathcal{B}_S(\beta H_i)$, where $H_i = J\langle s_i^z \rangle - \tilde{g}\mu_B H$ and $\mathcal{B}_S(x)$ is the Brillouin function. The process is iterated until self-consistency is achieved for all localized spins [11]. As a result, for a given random configuration of localized spins and fixed density of carriers n_e , we determine the chemical potential, μ , the energy, $E_{n\sigma}$, on the n -th level and the corresponding probability amplitude, $|\psi_{n\alpha,\sigma}(j)|^2$, for occupation of a carrier state with spin σ on a given site j on sublattice α . With these values, we extract the magnetizations of the localized and itinerant spins on each sublattice, M_α and m_α , respectively, and the DOS.

We have performed calculations for systems with up to $N=2 \times 65 \times 65$ sites, and used random distributions of magnetic impurities corresponding to a given spin concentration n_s ; from now on, all quantities should be understood as configurational averages taken in ensembles varying between 10 and 50 disorder realizations, which suffice to yield small enough error bars. As we are interested in the case where the Fermi level is close to the Dirac point, in the following we set $n_e = 1$ (one electron per carbon).

As a check of our scheme, we verified that calculations for full coverage of local moments ($n_s = 1$) at $\mu = 0$ correctly reproduce the AFM ground state predicted by perturbative methods [6, 7]; at low temperatures, our results also agree with those obtained through Monte-Carlo simulations with frozen charge degrees of freedom [9]. For a random distribution of impurities, Fig. 1(a) shows one localized spin configuration for $n_s < 1$ and $\mu = 0$; we see that both FM and AFM clusters are formed. The corresponding carrier DOS is depicted in Fig 1(c): a gap clearly opens around the Dirac point [14].

The mechanism of gap opening in this material strongly resembles the double-exchange mechanism in manganites [15]. Hopping does not flip the electron spin while it moves from one sublattice to another; since neighboring adatoms (occupying different sublattices) are antiferromagnetically aligned, it costs an energy J for an electron to move between sublattices, leading to electronic localization. In Fig. 1(d), we show the inverse participation ratio (IPR), which measures the degree of localization of states, and is defined by the quantity $P_{\sigma n} = \sum_{i\alpha}^N |\psi_{n\alpha,\sigma}(i)|^4$. For an extended state, $P_{\sigma n}$ scales with $1/N$, whereas for a true localized state it does

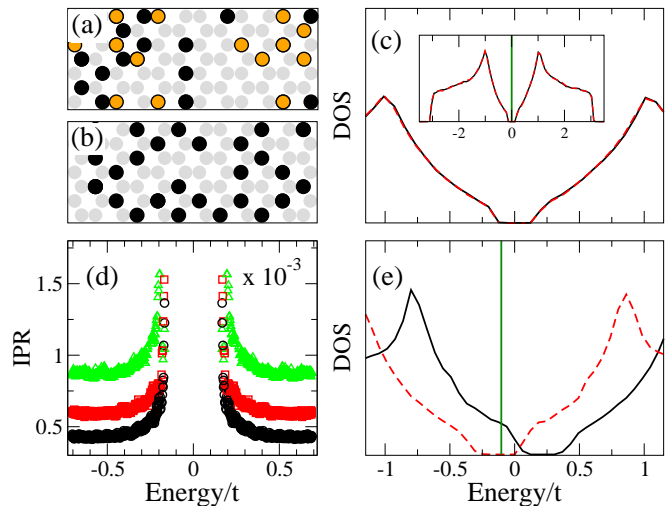


FIG. 1: (Color online) (a) and (b): Typical spin configuration (spin up in black, down in orange) for $n_s = 0.4$, $N = 2 \times 65 \times 65$: (a) spins of both sublattices ($\mu = 0$); (b) spins on one sublattice ($\mu = 0.105$); (c) and (e): density of states (DOS) averaged over disorder realizations represented by panels (a) and (b), respectively. Solid (dashed) lines represent spin up (down) electronic states. The inset in panel (c) shows the DOS over a wider energy range. Vertical lines indicate the Fermi level. (d) Inverse participation ratio (IPR) calculated under the same conditions as in (a) for three system sizes: $N = 4050$ (green triangles), $N = 6050$ (red squares) and $N = 8450$ (black circles); All data are for $J = t$, and $k_B T = 0.002t$.

not scale with the system size, and its IPR is comparatively larger. States near the gap have a significantly larger IPR than those with energies away from it; see Fig. 1(d). Therefore, the former states are localized, while the latter, whose IPR clearly scales with N , are extended. In the dilute limit, these localized states resemble self-trapped magnetic polarons, similar to the ones proposed by Nagaev [16]: carriers are localized by exchange interaction in spin-polarized droplets located at energetically favorable positions, whose sizes scale with $1/J$. Our numerics also indicates that the localization of the charge carriers is robust against local gating effects induced by the local reconstruction of the electronic density at the impurity sites. We considered this effect by adding a diagonal term in the graphene Hamiltonian that changes the on-site energy at sites where the magnetic ions are attached. We find that the gap is still present for on-site energies $\lesssim J$. Since the exchange coupling can be extremely large [13, 17], the localization effects discussed here may be dominant for a variety of adatoms in graphene.

If the spins are forced to occupy only one sublattice, as shown in Fig. 1(b), the ground state is FM, as expected [6, 7]. The spin degeneracy is lifted and the corresponding DOS for spin up and spin down carriers are shifted in opposite directions. Exactly at the Dirac point, the system is metallic, and the up and down spin popula-

tions compensate each other [14]. Away from half-filling the carriers are spin-polarized at the Fermi energy, as we show in Fig. 1(e). However, the use of this system as a source of spin-polarized carriers in graphene is hindered by the difficulty of controlling the deposition of adatoms in just one of the sublattices; one should therefore seek ways of producing spin-polarized carriers in a system without the need of controlling the specific position of the adatoms. In what follows, we consider only adatoms randomly located on *both* sublattices, as is the case in most experiments. As Fig. 1(c) illustrates, we can extract the magnitude of the gap from the density of states, for different temperatures, coverages, magnetic fields, and so forth, thus establishing quantitative correlations between magnetic and electronic properties, as we now discuss.

We first examine the behavior of the staggered magnetizations, $M_s = |M_A - M_B|/S$ and $m_s = |m_A - m_B|/s$, corresponding to local and itinerant spins, respectively. From Fig. 2(a), we see that due to the nature of the RKKY interaction in graphene, even for a diluted system with ferromagnetic clusters [see, e.g., Fig 1(a)], M_s attains its maximum value, n_s , at low temperatures. The spins of carriers and magnetic impurities are antiferromagnetically coupled to each other by the exchange interaction, and hence both magnetizations vanish at the same critical temperature T_c , for a given n_s Figure 2(b) shows the temperature dependence of the gap, $\Delta(T)$, from which the correlation between the curves in panels (a) and (b) is clear: Δ decreases from its saturated value (proportional to $n_s J$ [14]) at low T , tracking the behavior of both M_s and m_s , until it reaches a minimum value when $M_s = m_s \simeq 0$; due to the finiteness of the system, this minimum value is not zero, hence setting a minimum energy scale. Below T_c , the resistivity of the system displays an activated behavior, typical of a semiconductor for $k_B T \ll \Delta(T=0)$, but undergoes a metal-insulator (MI) transition at intermediate temperatures. The strong temperature dependence of the gap and the temperature-induced MI transition resemble the transport characteristics of Kondo insulators [18].

When a sufficiently strong magnetic field H_c is applied, aligning the local spins, electronic hopping is no longer hindered: the charge carriers delocalize, and the system becomes metallic. This behavior can be seen from Figs 2(c) and (d), which illustrate that for a fixed T , the gap also tracks the behavior of M_s with H : Δ vanishes when the spins in both sublattices point in the same direction. This dependence has important consequences for the transport properties of magnetically doped graphene: the system will display a very strong negative magnetoresistance, since H tends to close the gap and to increase dramatically the conductivity of the system. This effect is very similar to the one observed in manganites and in magnetic semiconductors, such as EuSe [15] and magnetic hexaborides [19]; it could also have bearings

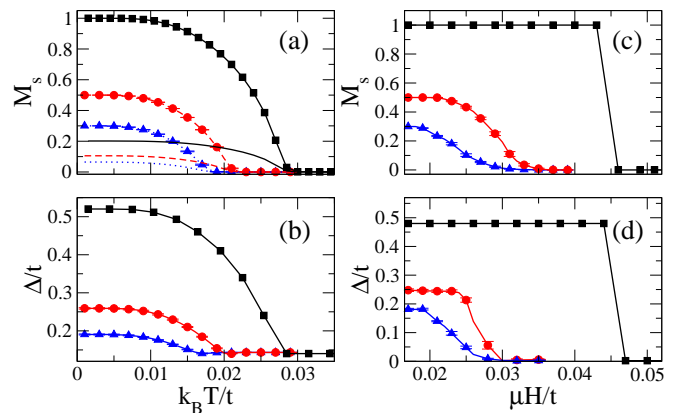


FIG. 2: (Color online) (a) Staggered magnetization versus temperature for localized spins and carriers and different impurity concentrations: $n_s = 1$ (black squares for M_s , and full line with no symbols for m_s), $n_s = 0.5$ (red circles and dashed line) and $n_s = 0.3$ (blue triangles and dotted line); (b) Gap Δ as a function of the temperature [the color code for n_s in (a) is the same in all panels]; (c) Staggered magnetization as a function of applied magnetic field H ; (d) Gap as a function of H . $J = 0.5t$, $\mu = 0$ and $N = 2 \times 50 \times 50$ in all cases.

on the colossal negative magnetoresistance observed in dilute fluorinated graphene [20].

As it can be seen from Fig. 2, magnetic field, temperature, and concentration of magnetic adatoms can be used to control the magnitude of the gap in graphene, since it tracks the staggered magnetization M_s . Therefore, in order to manipulate Δ , it is necessary to establish the range of parameters for which the gap opens or closes. To this end, we have varied n_s and determined the T_c and H_c (for fixed T); some of the results are summarized in Fig. 3. These critical lines depend on the value of J used, but this can be easily scaled since $T_c \propto J^2$ for $n_s = 1$, as seen from the inset of Fig. 3(a). The phase diagrams of Fig. 3 also illustrate that as one increases n_s , the carrier polarization tends to increase, which, in turn, enhances the effective coupling between local moments: T_c rises.

The external field breaks the degeneracy between spin-up and spin-down density of states (see Fig. 4). This is

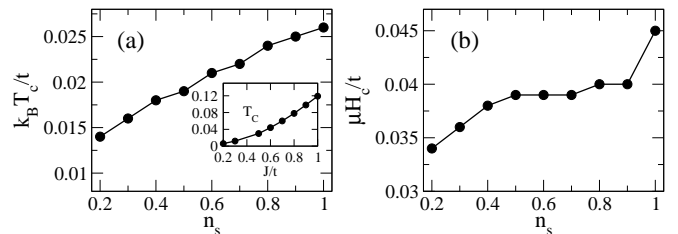


FIG. 3: (a) Critical temperature T_c ($M_s = 0$) versus spin concentration n_s . (b) Critical field T_c versus n_s for $T = 0.001t$. $J = 0.5t$. $N = 2 \times 36 \times 36$. The inset in panel (a) shows T_c in function of J .

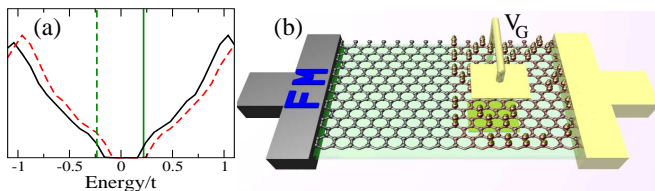


FIG. 4: (a) Electronic density of states for $J = t$, $n_s = 0.5$, $\mu H = 0.12t$, $k_B T = 0.001t$, and $\mu = \pm 0.1t$, where solid lines represent spin up and dashed lines spin down electronic states. Vertical lines indicate the Fermi level. A device using these features is sketched in (b); see text.

very similar to the case of spins in one sublattice discussed above (see Fig. 1(d)). Both the energy gap and the DOS are not strongly dependent of μ ; therefore, a small variation of μ , caused e.g., by a gate voltage, can drive the system from an insulator to a metallic regime with spin-polarized carriers, where only spin-up (or spin-down) states are available. Indeed, Fig. 4(a) shows the DOS for $\mu = 0$, indicating that the system is an insulator; for $\mu \simeq 0.1t$, Fig. 4(b) shows that there is a net occupation of spin-down (up) states at the Fermi level.

It is important to stress the fact that small variations of μ can change the transport properties of the system, while producing different imbalances of spin-up and spin-down available states, opens the possibility of generating and controlling spin-polarized currents through the use of randomly distributed adatoms in graphene. Further, differently from other spin-injection schemes experimentally tested [4], in this case injection has no external agents, thus eliminating unwanted sources of scattering such as interface mismatch between graphene and other materials, like magnetic metals.

In order to discuss how these peculiar properties can be used in devices, we first note that a single graphene layer can be separated in different regions with and without the presence of adatoms, if during the adatom deposition part of the layer is covered with a mask. As illustrated in Fig. 4(a), an external magnetic field induces the necessary spin imbalance in the DOS, and gate voltages V_G can be used to change the spin polarization of the available states at the Fermi level. With this in mind, we can produce and test spin polarized currents using a device sketched in Fig. 4(b). Half of the layer is covered with magnetic adatoms, with which a normal contact is made, while the clean part has a magnetic contact, such as Cobalt. An external field is turned on and produces the shift in DOS, while the gate voltage moves μ in either direction, as illustrated in Fig. 4(a). If a current passes through the system from the normal to the magnetic contact, spin-polarized currents are generated in the magnetically doped part of graphene and injected in the clean part. The polarization can be tested by the magnetic contact.

These ideas can also be used to propose a spintronics

device similar to a spin-valve [21]. Instead of separating the layer in two parts, as above, it is now separated in three: two magnetically doped parts separated by a clean one. The doped parts are subject to independent V_G 's and both have normal metallic contacts. With the same H and different V_G 's, each magnetic part can have a specific imbalance of available states at the Fermi Level. If a current passes through the system in both directions, the magnetoresistance can be controlled by the V_G 's. The device also produces spin-polarized carriers in one side, and tests the polarization in the other. In the calculations leading to Fig. 4(a), we have used large values of J and n for illustrative purposes only. In the device sketched in Fig. 4(b), for $n_s = 0.1$, and $J = 0.1$ eV, spin polarized carriers can be produced by fields less than 1T, combined with gate voltages of the order of a few mV.

In conclusion, we have established that a random distribution of magnetic adatoms can localize charge carriers and open a gap in graphene. The mechanism of gap opening is the hindering of hopping due to the antiferromagnetic correlation of magnetic impurities on opposite sublattices. The size of the gap depends on the concentration of adatoms, and on the strength of the exchange coupling; it can therefore be controlled by temperature and external magnetic field. These two adjustable parameters can drive graphene into a metal-insulator phase transition in the presence of magnetic disorder. Furthermore, we showed that a magnetic field can be used to produce spin polarized carriers, suitable for spin injection and other spintronic applications.

We thank E. Fradkin for discussions. The research by TGR, MG, and RRdS was supported by the Brazilian Agencies CNPq, CAPES, and FAPERJ; MG also acknowledges partial support from FAPEMAT. AHCN acknowledges the ONR grant MURI N00014-09-1-1063, and BU acknowledges partial support from the DOI grant DE-FG02-91ER45439 at University of Illinois.

-
- [1] K. S. Novoselov *et. al.*, Nature **438**, 197 (2005); Y. Zhang *et. al.*, Nature **438**, 201 (2005); A. H. Castro Neto *et. al.*, Rev. Mod. Phys. **81**, 109 (2009).
 - [2] B. Uchoa *et. al.*, Phys. Rev. Lett. **101**, 026805 (2008).
 - [3] O. V. Yazyev and L. Helm, Phys. Rev. B **75**, 125408(2007); A. V. Krasheninnikov *et. al.*, Phys. Rev. Lett. **102**, 126807 (2009); P. Venezuela *et al.*, Phys. Rev. B **80**, 241413 (2009); M. Wu *et al.*, Appl. Phys. Lett. **93**, 082504 (2008).
 - [4] N. Tombros *et al.*, Nature **448**, 571(2007).
 - [5] I. Zutic *et al.*, Rev. Mod. Phys. **76**, 323 (2004).
 - [6] S. Saremi, Phys. Rev. B **76**, 184430 (2007).
 - [7] L. Brey, *et al.*, Phys. Rev. Lett. **99**, 116802 (2007).
 - [8] A. M. Black-Schaffer, Phys. Rev. B **81**, 205416 (2010).
 - [9] T. G. Rappoport, B. Uchoa, A. H. Castro Neto, Phys. Rev. B **80**, 245408 (2009).
 - [10] A. C. Hewson, The Kondo Problem to Heavy-Fermions

- (Cambridge: Cambridge University Press, 1997).
- [11] M. Berciu and R. N. Bhatt, Phys. Rev. Lett. **87**, 107203 (2001).
 - [12] M. Berciu and R. N. Bhatt, Phys. Rev. B **69**, 045202 (2004).
 - [13] B. Uchoa, T. G. Rappoport and A. H. Castro Neto, arXiv:1006.2512.
 - [14] M. Daghofer, N. Zheng, A. Moreo, arXiv:1005.3726v1.
 - [15] E. Dagotto, T. Hotta, and A. Moreo, Phys. Rep. **344**, 1 (2001); J. M. D. Coey *et al.*, Advances in Physics **48**, 167 (1999).
 - [16] E. L. Nagaev, JETP Letters, **74**, 431 (2001).
 - [17] D. Jacob and G. Kotliar, Phys. Rev. B **82**, 085423 (2010).
 - [18] P. S. Riseborough, Adv. Phys. **49**, 257 (2000).
 - [19] V. M. Pereira *et al.*, Phys. Rev. Lett. **93**, 147202 (2004).
 - [20] X. Hong *et al.*, arXiv:1008.4387.
 - [21] M. N. Baibich *et al.*, Phys. Rev. Lett. **61**, 2472 (1988).